Infrared Reflectivity Spectroscopy of Optical Phonons in Short-period AlGaN/GaN Superlattices

J. B. Herzog, A. M. Mintairov, K. Sun, Y. Cao, D. Jena, J. L. Merz.

University of Notre Dame, Dept. of Electrical Engineering, Notre Dame, IN, USA;

ABSTRACT

GaN and AlN compounds have been proven useful in wide bandgap microelectronics and optoelectronics. Also properties of bulk GaN and AlN have been studied extensively. However, many characteristics of AlGaN/GaN superlattices are not well known. In particular, the properties of phonons have not been determined. In order to determine phonon properties, this study measured infrared reflectivity spectra on short period superlattices, which were grown by high quality molecular beam epitaxy. The superlattices consisted of 300 periods of alternating layers of GaN and AlGaN, each containing between 1 and 8 monolayers. Next, the reflectivity of each sample was measured using a Bruker IFS-66V spectrometer. From these experimental spectra the dielectric function, and hence the optical phonon properties (namely phonon frequency and phonon damping), were determined. Mapping the experimental spectra with theoretical calculations determined the longitudinal and transverse optical phonon energies present in the AlGaN/GaN superlattices. Through the examination of different AlGaN/GaN superlattice combinations, plots of phonon energies versus material composition were obtained. Furthermore, new phonons, that were not present in bulk AlN and GaN, were discovered. Finally, phonon characteristics were measured as a function of temperature, confirming that phonon energies decrease with increasing temperature.

Keywords: Infrared Reflectivity, Spectroscopy, Optical Phonons, Phonons, AlGaN/GaN, Superlattice

1. INTRODUCTION

Superlattice (SL) semiconductors are crystals grown with alternating atomic layers. The first superlattice was grown only thirty years ago. Since their creation, superlattices have been used in many optical and electronic applications. For example, superlattices are used as channels in high current and high power field effect transistors. Superlattices are used as a buffer layer in heterostructure devices to alleviate strain. Quantum Cascade Lasers, Bloch Oscillator devices, and Avalanche Photo Diodes also contain superlattices. Some of the latest superlattice applications include superlattice solar cells and Ultra-fast optical switches.[1]

Phonons, which are atomic vibrational waves, greatly affect electron mobility due to scattering. Phonons can be longitudinal or transverse waves. These waves displace atoms in semiconductor crystals which in turn alter the electronic potential and cause electron scattering. In compound semiconductors, like AlN and GaN, the bond is ionic. This dipole of different atoms oscillating in opposite directions creates an optical phonon which produces an electric field. Due to these polar optical phonons, the electric field causes very strong scattering, which is typically the dominating scattering mechanism in compound semiconductors.[2] The effects of phonons are not always negative as in the instance of impeding electron mobility. Phonons can be useful in dissipating heat out of semiconductors.

Many studies have analyzed phonon properties in Bulk GaN and AlN,[3] and a number of studies have also examined superlattices such as AlAs/GaAs. The purpose of the current study is to further superlattice phonon research by examining the phonon characteristics of AlGaN/GaN superlattices.

email: jherzog1@nd.edu

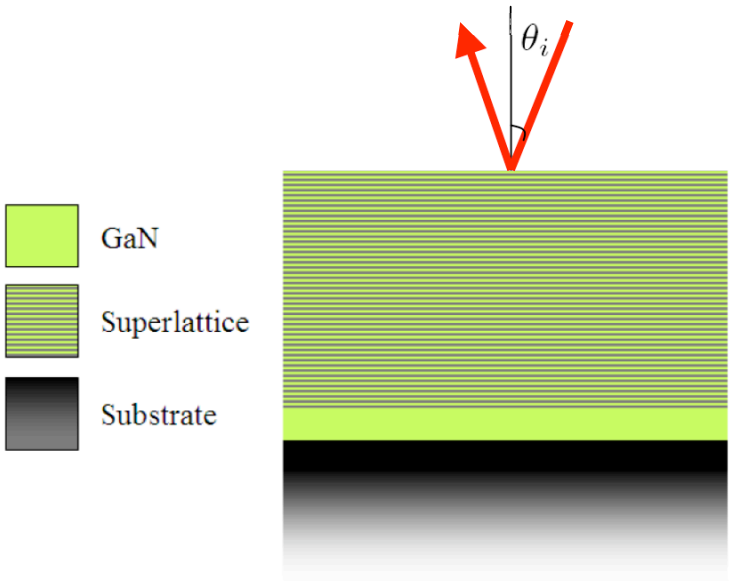

Figure 1. Cross section of a sample: superlattice grown on a sapphire substrate. A 30nm GaN buffer is between the superlattice and the substrate. Also illustrated is the reflectivity angle of 15 degrees.

2. SUPERLATTICE STRUCTURE

The AlGaN/GaN superlattices in this work have been grown by molecular beam epitaxy (MBE) at the University of Notre Dame. First, a thin (30-70nm) GaN buffer layer was deposited on a sapphire substrate. Then the superlattice made of 300 short periods was grown on this buffer layer. A cross section of a standard sample is shown in Fig. 1. A short period consist of n monolayers of AlGaN plus m monolayers of GaN, where $0 < m, n \leq 8$. Six different superlattices samples were studied which vary in layer thickness and thickness ratio. They are summarized in Table 1. X-ray diffraction measurements confirmed structure composition by using Xpert Epitaxy software to verify the aluminum concentration of each sample.

Table 1. Aluminum concentration, period monolayer composition, and period length of each superlattice sample. Each superlattice consists of 300 periods and each period consists of $n + m$ monolayers.

Sample Name	**Al concentration** (%)	**AlGaN:GaN** (n:m)	**Period Length** (nm)
092505b	10.0	2:8	2.5
091805	16.5	1:2	0.75
092505a	25.0	4:4	2
091605	25.5	2:2	1
092705	36.0	2:1	0.75
092605	42.0	8:2	2.5

3. EXPERIMENTAL PROCEDURE

Room and low temperature infrared reflectivity spectroscopy measurements were taken on each superlattice sample using the Bruker IFS-66V Fourier Transform Infrared (FTIR) spectrometer. The measurements were in the infrared wavenumber range of $400cm^{-1}$ to $2000cm^{-1}$ because the optical phonons of interest were also contained in this region. The reflection angle of incident, shown in Fig. 1, was held constant at 15^{o} in order to minimize the number of variables but also because of the geometric constraints of the cryostat. Low and room temperature measurements were conducted inside a cryostat. Room temperature measurements were also performed without the cryostat to verify that the cryostat did not bias the results.

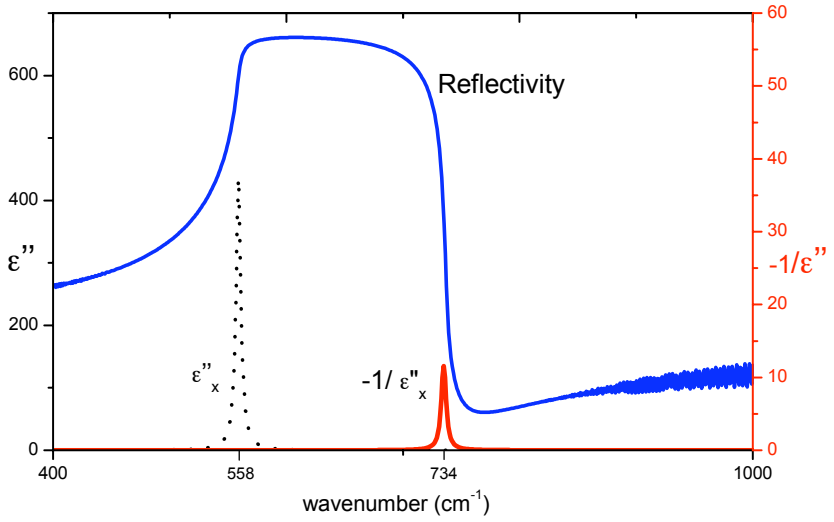

Figure 2. Reflection spectrum of bulk GaN calculated with the plotted dielectric function $\epsilon''(\omega)$ and $-1/\epsilon''(\omega)$. The optical phonon frequencies of GaN are shown on the x-axis in wavenumber $\tilde{\nu} = \omega/c$. The reflectivity y-axis $(0 < y \leq 1)$ is not shown.

4. THEORY

Calculating the dielectric function of the semiconductor material is the foundation in relating phonon frequencies to the reflectivity spectrum. This is accomplished using the expression

$$\epsilon(\omega) = \epsilon_\infty + \sum_{j=1}^{m} \frac{4\pi F_j}{\omega_{Tj}^2 - \omega^2 - i\omega\gamma_{Tj}}\,, \tag{1}$$

where ϵ_∞ is the high-frequency dielectric constant and F_j, ω_{Tj}, and γ_{Tj} are the jth-mode oscillator strength, transverse optical (TO) phonon frequency, and damping respectively. Oscillator strength is also a function of transverse and longitudinal optical (LO) phonon frequencies:[4]

$$F_j = \frac{\epsilon_\infty}{4\pi}(\omega_{Lj}^2 - \omega_{Tj}^2) \prod_{k\neq j}^{m} \frac{\omega_{Lk}^2 - \omega_{Tj}^2}{\omega_{Tk}^2 - \omega_{Tj}^2}\,. \tag{2}$$

In general, the dielectric function can be separated into real and imaginary parts, $\epsilon(\omega) = \epsilon'(\omega) + i\epsilon''(\omega)$. The imaginary part of the dielectric function $\epsilon''(\omega)$ is the energy absorbed as a function of frequency and therefore directly affects the reflectivity spectrum of that material.[5]

Fig. 2 shows a simple example of how optical phonons frequencies of bulk GaN affect the imaginary part of the dielectric function, $\epsilon''(\omega)$, by plotting this function. The transverse optical (TO) phonon is at $558_x cm^{-1}$, and the longitudinal optical (LO) phonon in GaN is at $734_x cm^{-1}$. These phonons frequencies are where the dielectric functions $\epsilon''(\omega)$ and $-1/\epsilon''(\omega)$ peak. Shown in the GaN spectrum, light with frequencies between the TO and LO phonons has high reflectivity. The spectrum is the total unpolarized reflectivity $\mathcal{R}_u$ which was calculated from the s- and p-polarized reflectivity components:[6]

$$\mathcal{R}_s(\omega) \quad = \quad \left| \frac{\cos\theta_i - [\epsilon_x(\omega) - (\sin^2\theta_i)]^{\frac{1}{2}}}{\cos\theta_i + [\epsilon_x(\omega) - (\sin^2\theta_i)]^{\frac{1}{2}}} \right|^2\,, \tag{3}$$

$$\mathcal{R}_p(\omega) = \left| \frac{\epsilon_x^{\frac{1}{2}}(\omega)\cos\theta_i - [1-(\sin^2\theta_i)/\epsilon_z(\omega)]^{\frac{1}{2}}}{\epsilon_x^{\frac{1}{2}}(\omega)\cos\theta_i + [1-(\sin^2\theta_i)/\epsilon_z(\omega)]^{\frac{1}{2}}} \right|^2 , \quad (4)$$

$$\mathcal{R}_u(\omega) = \frac{1}{2}\Big(\mathcal{R}_s(\omega) + \mathcal{R}_p(\omega)\Big) . \quad (5)$$

For bulk materials, the reflection spectrum is calculated with Eq. (3), (4), and (5). Notice in these equations that the reflectivity spectrum is strongly dependant on the dielectric function. Fig. 2 graphically illustrates how the reflectivity, the dielectric function, and phonon frequencies are related.

The reflectivity spectrum calculation become more complex in thin multilayered semiconductors due to the interfaces between the different materials that make up the sample. For some simplicity, the superlattice (SL) is approximated to be one layer, reducing the sample to three thin layers: SL, GaN buffer, and sapphire substrate. Reflectivity due to each layer is calculated from Eq. (3), (4), and (5) as in bulk materials. The total multilayered reflectivity spectra are then computed from these results, as described in detail in Ref. 6. Fig. 3 shows the total multilayered reflectivity spectrum. Comparing Fig. 3 to Fig. 2 shows the similarities and additional complexities that arise in the multilayered structures.

5. MAPPING

The optical phonon energies were obtained from the reflectivity spectrum of the superlattice by using the equations previously outlined. Mapping was used to match the calculated theoretical spectrum with the measured experimental spectrum. Many inputs were used in order to calculate the reflectivity spectrum. Some of the inputs are the phonon energies of the substrate and the buffer layer. The phonon energies of these layers are given and are used to calculate the dielectric function. The dielectric function of these two layers, shown in the top graph of Fig. 3, are held constant during mapping. The superlattice dielectric function on the other hand, which is shown in the middle plot of Fig. 3, is varied by changing the frequencies of the optical phonons of the superlattice.

Changing the superlattice dielectric function alters the theoretical reflectivity spectrum. The superlattice phonon energies are therefore adjusted until the theoretical calculations match the infrared spectrum experimental results. The lower plot of Fig. 3 shows the best mapping of this theoretical calculation with experimental results. The local minima of experimental and theoretical spectra are the critical frequencies that are matched by tuning the SL phonon frequencies. Note that the strong reflectivity between 440-480cm^{-1} is due to the sapphire substrate. The substrate's transverse and longitudinal phonons at those frequencies plotted in the upper graph form this reflected band. Since the substrate parameters are held constant and affect the low wavenumber range, the local minima less than 500cm^{-1} do not need to match with theoretical results. The low energies of the spectrum are also not of interest in determining characteristics of phonons in the SL since phonon frequencies in the SL are greater than 500cm^{-1}. In the region below 500cm^{-1}, a shift in the minima between the theoretical and experimental plots exists. This misalignment could be due to strain in the substrate caused by the superlattice. The high reflectivity range from 550-740cm^{-1} is primarily from GaN (as shown in Fig. 2), but much of the additional structure in the reflectivity arises from SL phonons, especially in the 500-600cm^{-1} range.

6. RESULTS

Room temperature experiments were conducted to determine the phonon energies as a function of aluminum concentration and the number of phonons that exist in each sample. Next low temperature experiments were preformed to see how these phonon energies were affected by change in temperature.

6.1. Room Temperature Results

All six superlattice samples were mapped to determine the optical phonon that exist at room temperature in the superlattice structure. Fig. 4 shows how all the phonons in each sample are related and how each sample also have similar phonons to bulk AlN and GaN. Bulk AlN has optical phonons at approximately 900 cm^{-1} and 660 cm^{-1} as shown on the right side of the graph while bulk GaN has optical phonons near 558 cm^{-1} and

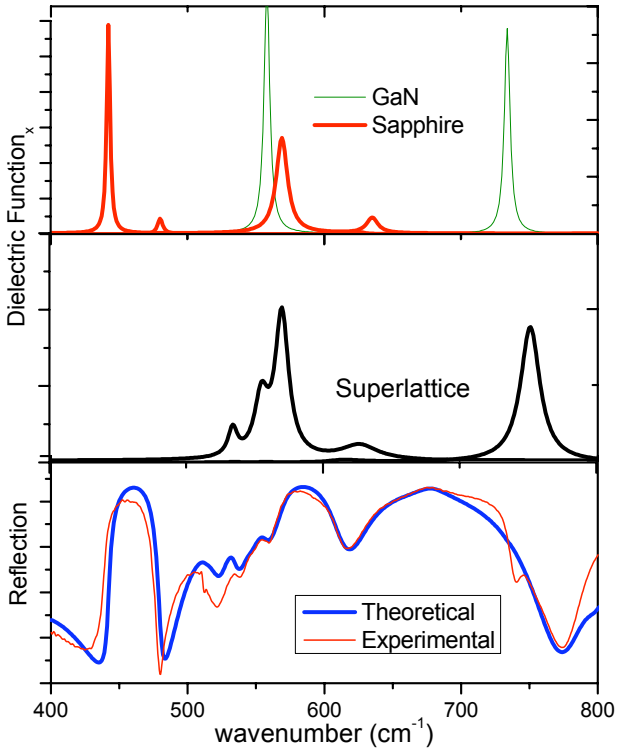

Figure 3. Top graph displays the dielectric functions $\epsilon_x''(\omega)$ and $-1/\epsilon_x''(\omega)$ of the GaN buffer layer and the sapphire substrate, the parameters of which are held constant during calculations of the reflectivity. The middle graph contains the superlattice dielectric functions, which will also be used to calculate the reflectivity. The lower graph displays both the calculated theoretical reflectivity and experimental measurements. During mapping, the superlattice dielectric functions are adjusted by changing the superlattice optical phonon energies until the theoretical reflectivity and experimental results match appropriately.

734 cm^{-1} (plotted on left). Note that an additional phonon, e(1a), exists only in the superlattice samples, but does not exist in the bulk materials. This phenomenon of a new phonon also has been observed in AlAs/GaAs superlattices.

6.2. Low Temperature Results

The low temperature reflectivity spectra were studied on the superlattice samples. In Fig. 5 one can see that the minima of the reflectivity shift towards higher energy as the temperature decreases. This shift in the minima corresponds to a shift in the phonon energies. The reflectivity at each temperature was mapped to determine the phonon energy at each temperature. The results of the optical phonon energies versus temperature are plotted in Fig. 6. This shift is to be expected because as the temperatures decrease, the distance between atoms decreases causing the bonds between each atomic pair to become stronger. This stronger bond can be thought of as a spring constant and is proportional to the frequency of oscillation or in other words, the phonon energy. These results show that optical phonon energy decrease exponentially as temperature increases and also match GaN results in literature.[7] Plotted in Fig. 6 are the phonon energies of sanple 091605 which is the sample with 25.5% aluminum. Also labeled are the optical phonons that are present in the superlattice corresponding with Fig. 4. The data points are approximated with a least square fit which is the solid line. This approximation is also what is shown for bulk GaN phonon temperature dependance.[7]

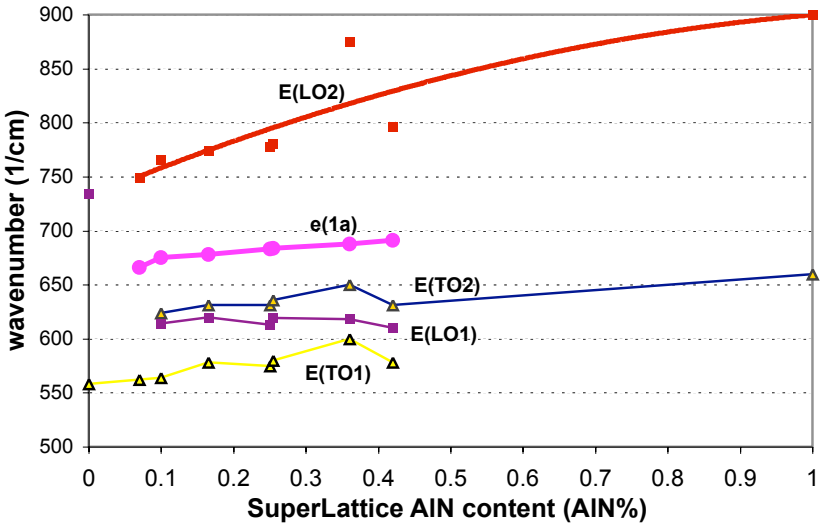

Figure 4. Optical phonon energies in each AlGaN/GaN sample at room temperature as a function of aluminum concentration. Each vertical set of data represents the phonons present in a single sample. Plotted on the edges are the phonon modes in bulk AlN and GaN. Notice the phonon e(1a) which is a new phonon that exists in the superlattices but not in the bulk.

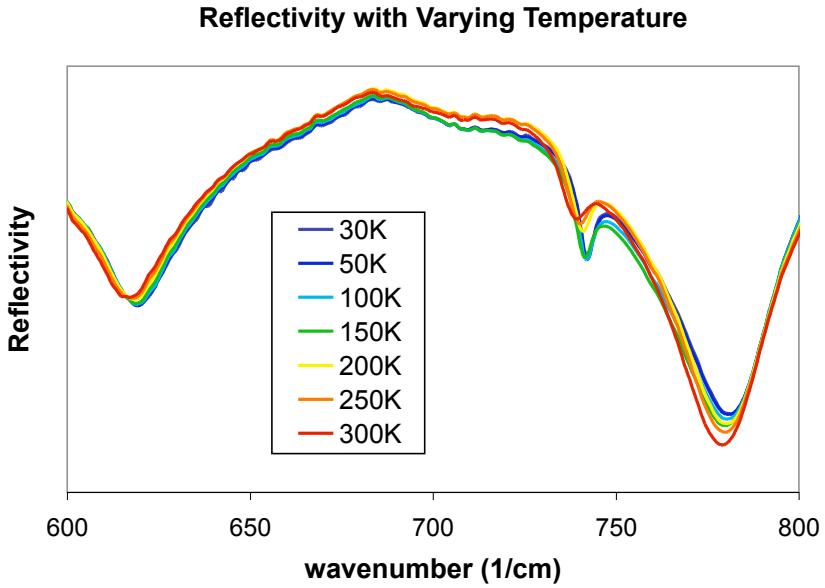

Figure 5. The varying reflectivity of sample 092505b as a function of temperature. These spectra are shown in the range from 600-800 cm^{-1} in order for the shift in the minima to be observed. This temperature dependance on the minima of the reflectivity results in a phonon energy dependancy on temperature.

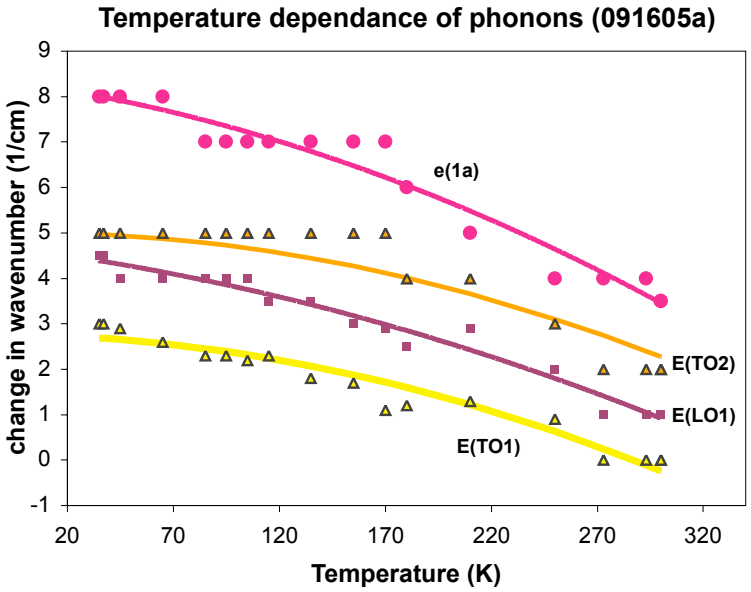

Figure 6. The optical phonon energy of sample 091605a as a function of temperature. Each vertical set of data represent a single spectrum mapping to give the phonon frequencies at that specific temperature. The phonon labels correspond to Fig. 4. The lines are the least square fit approximation of each phonon temperature dependance. The least square fit is also an approximation for the phonon energy dependance in bulk GaN.[7]

7. CONCLUSIONS AND FUTURE WORK

7.1. Conclusions

With the use of infrared reflectivity spectroscopy, the phonon energies in the AlGaN/GaN superlattices of this study have been determined. The optical phonon frequencies have been plotted as a function of aluminum concentration in order to observe the energy shift with the change in aluminum concentration. Another significant finding of the study is the observation of a new phonon frequency in the superlattice sample that does not correspond to any of the native phonon energies that are present in the bulk materials. This new phonon is similar to a new phonon occurrence in other compound semiconductors.

Temperature dependance of phonon energies have also been measured in this work. It has been discovered that AlGaN/GaN superlattice phonon frequencies increase as temperature decreases. This matches the same trend as in bulk GaN as expected.

7.2. Future Work

The future direction of this research is to study additional superlattice samples in order to continue to characterize optical phonon properties. Another direction will be to study AlN/GaN superlattices in order to observe the phonons that are present in these superlattices, specifically the new phonon that does not exist in the bulk materials. Future studies will examine what specifically causes these new modes.

ACKNOWLEDGMENTS

I would like to thank Sasha (A. Mintairov) for teaching me about superlattices and optical phonons and for always being willing to answer my questions. I would like to thank Kai Sun for instructing and training me on lab equipment, especially on the FTIR spectrometer. I would like to thank Yu Cao for helping me with the X-ray measurements and for providing the samples. Also I would like to thank Dr. Jena, who runs the MBE lab, for providing the samples and exciting my interests in the future of wide bandgap semiconductors. I would also like to thank Trish Snell for editing this paper. Finally, last but not least, I would like to thank my advisor,

Dr. J. Merz, for taking me in, trusting in me, and motivating me. Thank you also Dr. Merz for your support, financial and otherwise.

REFERENCES

1. F. Guillot, E. Bellet-Amalric, E. Monroy, M. Tchernycheva, L. Nevou, L. Doyennette, F. H. Julien, L. S. Dang, T. Remmele, M. Albrecht, T. Shibata, and M. Tanaka, "Si-doped GaN/AlN quantum dot superlattices for optoelectronics at telecommunication wavelengths," *J. Appl. Phys.* **100**, p. 044326, 2006.
2. M. Lundsrom, *Fundamentals of Carrier Transport*, Cambridge, 2000.
3. A. S. Barker and M. Ilegems, "Infrared lattice vibrations and free-electron dispersion in GaN," *Phys. Rev. B* **7**(2), p. 743, 1973.
4. C. T. Kirk, "Quantitative analysis of the effect of disorder-induced mode coupling on infrared absorption in silica," *Phys. Rev.* **38**(2), pp. 1255–1273, 1998.
5. J. Merz, "Electromagnetic theory." electromagnetic theory lecture notes.
6. O. E. Piro, "Optical properties, reflectance, and transmittance of anisotropic absorbing crystal plates," *Phys. Rev. B* **36**(6), pp. 3427–3435, 1987.
7. W. S. Li, Z. X. Shen, Z. C. Feng, and S. J. Chua, "Temperature dependence of raman scattering in hexagonal gallium nitride films," *J. Appl. Phys.* **87**, pp. 3332–3337, 2000.